Optimization of Lung CT Image Processing and Recognition Based on E-SRG Segmentation Algorithm

Hongfei Ren*

University of Malaya, Kuala Lumpur, Malaysia

Abstract. Intelligent algorithms such as deep learning and parallel processing technologies such as mobile clouds are constantly evolving, heralding a new era of intelligence. In the new historical period, the development of intelligent medicine is facing great challenges and opportunities. In traditional medicine, medical imaging includes medical imaging and pathological imaging, which is an important reference for doctors in disease diagnosis. Image processing and recognition, as one of the key technologies of computer vision, must be improved under the premise of meeting the needs in practical applications. Therefore, according to the unique pathological characteristics of medical images, combined with the real-time and accuracy of images, the auxiliary diagnosis of images is the need of the development of intelligent medicine. The preprocessing technique and E-SRG algorithm used in this paper can improve the quality of images without being limited by the size of the dataset, and realize the complete segmentation of organs and tissues.

1. Introduction

The processing and recognition of medical image is an important part of medical image, which not only adapts to the accuracy and real-time of medical image, but also adapts to the characteristics of medical image itself. Through the analysis of the medical image quality problems, and puts forward the corresponding pretreatment method, selection and perfect the accord with the characteristics of pathological image segmentation algorithm, on the premise of raising the speed of the convolutional neural network, realizes the accurate segmentation of the target area, improve the speed of the convolutional neural network, this is a very effective method, can guarantee accuracy and real-time performance.

2. Medical image processing and recognition

2.1 Medical images and their features

Medical imaging has a variety of characteristics, which can be summarized into four types:

2.1.1 High noise interference

Noise in conventional imaging comes from external perturbations during photography and imaging. The acquisition mode of medical images is complex, and the condition of detection equipment and the distribution of pathological staining will have a certain impact on the imaging of images.

2.1.2 Complex background

The human body is an organic whole of interwoven organs, tissues, and structures. Therefore, the background of medical imaging is much more complex than that of other types of imaging. For example, CT scans include not only lung, but also bone, subcutaneous fat, etc. Pathological imaging is much more complex, including a large number of body fluids and other non-target cells. In addition, since there is usually no clear boundary between the background and the object in medical images, the features of the figure, such as the edge of the region, are also blurred [1].

2.1.3 Strong feature specificity of different images

There are certain individual differences in medical images. Medical images from different tissues have their own characteristics, and their morphological diversity will also be caused by the reasons of diseases. In addition, the imaging and pathological images of the lesions in the same patient show different imaging effects due to the difference of examination methods. Therefore, the characteristics of medical imaging are highly specialized.

* Corresponding author: E-mail: 1280538273@qq.com

2.1.4 High resolution

The definition of medical image is usually higher than the general image, that is, each area of the image contains more pixel points, as an input image of the image, its size is larger than the general image size [2].

2.2 Image recognition based on convolutional neural networks

Convolutional neural network is a typical neural network model. The LeNet-5 model is designed to solve the problem of handwritten digit recognition, which breaks through the research bottleneck of traditional neural networks and establishes a general convolutional neural network framework, it can be clearly seen in Figure 1.

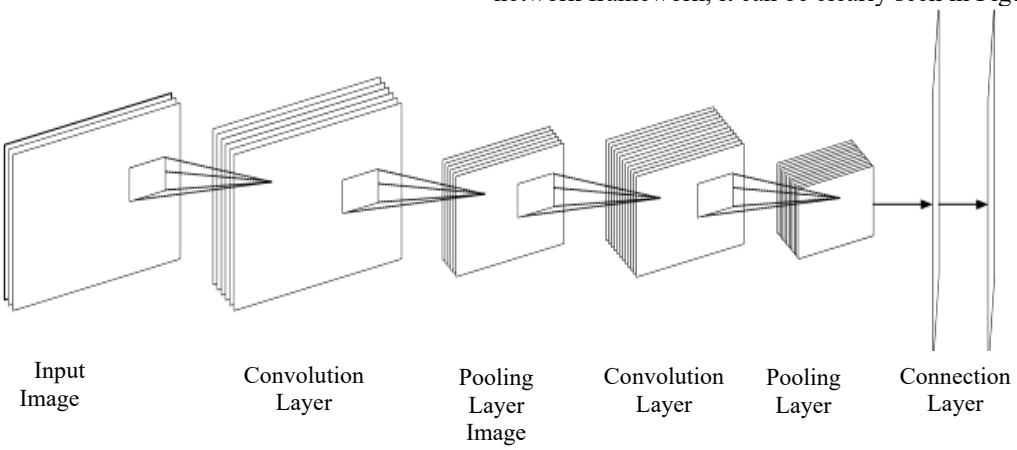

Figure 1 C ra

Convolutional layer is a key part of convolutional neural network, which can extract features from the input image. The convolution is calculated by summing the convolution kernel and the corresponding pixels in the perception region of the input image. Each convolution core has different size and weight, through sliding, convolution and other methods to extract various features of the image, and through the backward propagation, the weighted processing, gradually realize the feature fitting of the input image, so as to realize the accurate recognition of the image.

2.3 Intelligent imaging diagnosis

Intelligent medicine is a new technology that combines traditional medicine with artificial intelligence, which has penetrated into all aspects of the medical field. The application of this technology can effectively reduce the disparity of doctor-patient ratio and improve the work efficiency of medical staff. Traditional diagnostic methods require doctors to accumulate experience in clinical practice, while the combination of intelligent medical system and related technologies can achieve the functions of prediction before diagnosis, assistance during diagnosis, and supervision after diagnosis. Intelligent image diagnosis is the beginning of artificial intelligence in the field of medicine. By combining with computer vision technology, the accuracy of diagnosis can be effectively improved and the burden of diagnosis on medical staff can be reduced. The whole intelligent video system includes acquisition, display, processor and control parts, its core is to process and recognize the image. Medical diagnosis needs to be both rigorous and real-time.[6] Compared with other image processing and recognition, accurate and efficient processing and recognition are requ ver, the noise and background interference in medical images will seriously affect the image processing and recognition accuracy. However, high-resolution images not only restrict the speed of image recognition, but also require higher device performance. Therefore, the characteristics of medical images must be combined to improve the efficiency of their processing and recognition.[7]

3. Pulmonary CT image processing and analysis

Based on the lung CT images, the image preprocessing and E-SRG images were tested. The CT image data were obtained from LUNA16 (Lung nodule Analysis 16), which was collected from the Lung Nodule Test Competition data collection published by LIDC-IDRI in 2016. Images within the LIDC_IDRI image collection were removed from LUNA16 images, image inconsistencies and local losses were removed, and 888 CT images were saved. The data set includes imaging data (seg-lungs-LUNA16) and labeling data (CSVFILES). On this basis, the common Dicom format in medical images is converted into MHD and RAW formats, which are easy to manipulate. MHD contains the titles related to RAW images, such as the size of the picture, the date of shooting, etc. [8]

3.1 Pulmonary CT image preprocessing

The images in the dataset were first visualized to obtain the lung CT images in Figure 2. From the image, it can be seen that there is random black and white noise due to the presence of salt and pepper noise, and the edges are

relatively blurred. In order to obtain higher quality CT images, a preprocessing algorithm based on 55x neighborhood fuzzy boundary is used in this paper. In the middle pixel point, the influence of different neighboring pixel points on it decreases from inside to outside, and the final new pixel point and the original pixel point should be of the same magnitude, so the values of other parameters are: A value is 0.4, the inner adjacent value is 0.2, and the outermost layer is β=0.05. Secondly, under the premise of ensuring the clarity of the edges, appropriate noise reduction is carried out, and the selected neighborhood region should be 33x neighborhood. Then, the preprocessed CT images are shown in the figure.[9]

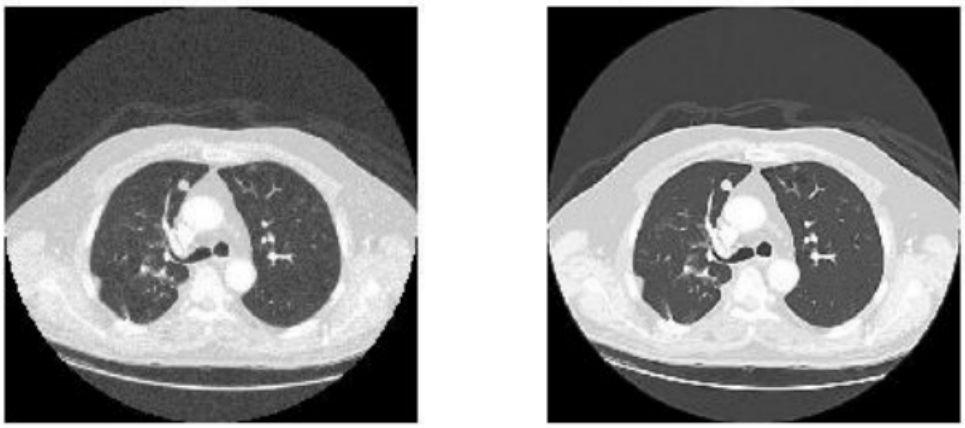

(a) Original CT images (b) Pre-processed CT images

Figure 2 Pulmonary CT image preprocessing

3.2 Simulation and result analysis of E-SRG segmentation of lung CT

In order to verify that the E-SRG algorithm can automatically and objectively select the seed region, this paper uses the automatic seed area growing algorithm and E-SRG algorithm to realize the seed point distribution based on the preprocessing of lung CT images. Figure 3 (a) is the pre-processed image, (b) is the seed point distribution of automatic seed area growth (SRG), (c) is the seed point distribution of E-SRG (E-SRG), and the seed points in (b) and (c) are black, respectively, while those not seeded are white. In order to prevent the use of manually intercepted non-black background in CT images from interfering with the seed point threshold setting of the seed region growing algorithm, the method was verified and the results are shown in Figure 4. As shown in Figs. 3 and 4, in the seed region growing algorithm, on the basis of no seed points, the seed regions selected by E-SRG are uniformly distributed in all seed regions, and the region composed by the seed points can reflect the overall contour of the whole image. Even if the influence of black background is removed, the method cannot reasonably select the seed points. The results show that when the regional gray level is high, the method cannot correctly select the seed points, that is, the method implemented by computer cannot realize the segmentation of CT images. So, in the later comparison simulations, we use artificially selected seed points and compare them using region growing algorithm[10].

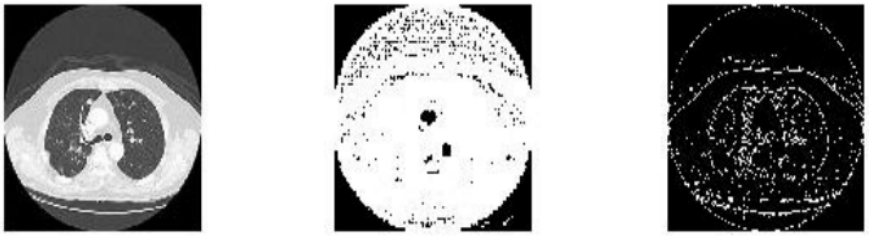

(a) Pre-processed CT image (b) Automatic SRG seed point distribution map (c)E-SRG seed point distribution map

Figure 3 Distribution of seed points

(a) Pre-processed CT image (b) Automatic SRG seed point distribution map (c) E-SRG seed point distribution map

Figure 4 Schematic representation of seed point distribution excluding background interference factors

3. E-SRG segmentation algorithm based on spatial correlation

1. Selection of seed areas

Step (1) Based on the gray level information of each pixel in the original image, integrate the spatial correlation of the region and generate the distance mapping matrix according to Formula 1:

$$D_i = \left[\left(x_i, y_i\right) - \frac{1}{N} \sum_{I_R \in N_R} \left(x_R, y_R\right) \right]^{\gamma} \tag{1}$$

The discussion point in the original figure is still Ii=(xi,yi). The discussion point in the corresponding distance mapping matrix is Di=(xi,yi)′NR represents the neighborhood pixel set of (xi,yi), (xR,yR) is the pixel in the neighborhood set, N is the number of pixels in the neighborhood, and y is the order moment coefficient.

It can be seen from the formula that the distance mapping matrix Di represents the γ moment of the gray mean value of the pixel in question and its neighborhood pixel in the original image. Since the average gray value of neighborhood pixels reflects the average gray value of pixels in the area, the elements in the distance mapping matrix can reflect the difference between the discussion point and its neighborhood pixels. This method not only retains the gray value information in the original image, but also reasonably adds the spatial correlation factor of the neighborhood difference.

Since the difference between the gray mean value of the discussion point and the neighborhood pixel is positive or negative, if γ is even, the negative difference will be assimilated into positive difference, which weakens the difference feedback to a certain extent. However, if γ is odd, the positive and negative differences can be completely preserved, so the order moment coefficient γ should be selected as odd. In addition, the larger the power coefficient y of the difference, the more drastic the difference reflected by the elements in the distance mapping matrix. So the order moment coefficient γ is hard to be over large. Since the third moment represents the skewness between random variables in the matrix, the order moment coefficient γ=3 in general.

Step (2) Based on the distance mapping matrix, the Otsu algorithm was used to calculate the distance-Otsu threshold as T according to the formula.

The difference within each region in the image is small, and the difference between regions (the boundary region) is large. Since the distance mapping matrix reflects the spatial difference relationship of pixels, the distance difference can be reasonably divided by the range-Otsu threshold based on the distance mapping matrix. Let the values of elements within the distance mapping matrix be $\triangle_K$ and the corresponding number be $n_{K\circ}$:

$$p_k = \frac{n_k}{\sum n_k} \tag{2}$$

$$\omega_1 = \sum_{(\Delta_k)_{\min}}^{T} p_k \tag{3}$$

$$\omega_2 = 1 - \omega_1 \tag{4}$$

Where, p_K in Eq. 2 is the frequency of the difference value $\triangle_K$ occurring in the distance mapping matrix, and $\omega_1$andω_2 in Eq. 3 and 4 are the sum of probabilities when the threshold is T, respectively. We have the mean as shown in Equations 5 and 6:

$$\mu_1 = \sum_{(\Delta_k)_{\min}}^{T} \Delta_k \frac{p_k}{\omega_1} \tag{5}$$

$$\mu_2 = \sum_{T}^{(\Delta_k)_{\max}} \Delta_k \frac{p_k}{\omega_2} \tag{6}$$

And the mean value of the whole image is shown in

$$\mu = \sum_{(\Delta_k)_{\min}}^{(\Delta_k)_{\max}} \Delta_k p_k \tag{7}$$

The variance is shown in Eq. 8 and 9:

$$\sigma_1^2 = \sum_{(\Delta_k)_{\min}}^{T} \left(\Delta_k - \mu_1\right)^2 \frac{p_k}{\omega_1} \tag{8}$$

$$\sigma_2^2 = \sum_{T}^{(\Delta_k)_{\max}} \left(\Delta_k - \mu_2\right)^2 \frac{p_k}{\omega_2} \tag{9}$$

Then the within-class variance and between-class variance of the distance mapping matrix are respectively:

$$\sigma_W^2 = \omega_1 \sigma_1^2 + \omega_2 \sigma_2^2$$

$$\sigma_B^2 = \omega_1 \left(\mu_1 - \mu\right)^2 + \omega_2 \left(\mu_2 - \mu\right)^2$$

Since the between-class variance is a first-order statistic based on the mean, the distance-Otsu threshold is the corresponding t-value when the between-class variance is maximized, $T = T_{\sigma_{\delta\max}^2}$

Step (3) Compare the elements in the distance mapping matrix with the threshold value T: if the element value is less than T, it is selected as the seed point. Otherwise, it is not selected as a seed point.

Distance mapping reflects the spatial difference of the neighborhood of the original gray scale map. Therefore, the pixels in the region of the original map have high similarity and small value of the mapped elements, which can be used as seed points representing the characteristics of the region. However, the regions with low boundary or similarity in the original image cannot be selected as seed points because they contain more gray level jump points and the mapped distance matrix elements have large values.

2. Regional growth

Step (4) Region growing based on distance mapping matrix. For a non-seed point, if all its four neighbors are seed points, the point is classified as within the corresponding region, and the complete growth is judged in turn.

All elements in the distance matrix mapped by pixels with high similarity in the region in the original image are selected as seed points. Therefore, the seed points selected according to steps (1), (2) and (3) often have regionality, that is, the final selected one is the seed region. In the traditional region growing algorithm, if the number of seed points is too large, the distance calculation between non-seed points and seed points will increase, resulting in too much calculation of the algorithm. In the E-SRG segmentation algorithm, almost all the pixels with high similarity in the region are selected into the seed region, and the regional characteristics of the seed points will reduce the calculation amount in the distance comparison process, and finally realize the simplified growth process.

Finally, the segmentation process based on E-SRG can be roughly divided into two parts: seed region selection and region growth. Specifically, it can be divided into four steps: distance matrix mapping during seed point selection, distance Otsu threshold calculation, comparison and selection of seed regions, and pixel region discrimination during region growth.

The E-SRG segmentation algorithm integrates spatial correlation on the basis of retaining gray information, and can reasonably segment images with complex gray levels in the region. In addition, because the selected seed points have regional characteristics, it can effectively reduce the calculation amount during the growth process. In addition, the algorithm does not rely on the pixel-level labels of the dataset, nor does it need the training and optimization of complex networks to complete the segmentation of medical images of any size. In conclusion, the E-SRG algorithm can achieve objective segmentation of complex medical images in a simple way.

In order to test the segmentation effect of E-SRG, this paper uses the seed region growing algorithm based on ESRG and combines it with E-SRG algorithm to segment lung CT images. Figure 5 (a) shows the preprocessed image, (b) shows the segmentation results of the seed region growing algorithm, and (c) shows the segmentation results of the E-SRG algorithm. Since the method to manually select the seed regions is to manually select the seed points, the lung lobes were manually selected, and the final segmentation result was only lung tissue and nothing else. As shown in Figure 5, although the seed region growing algorithm can generally realize the division of lung regions, the bronchi of the lung and the lower left part of the lung cannot be divided into target regions, and the trachea and blood vessels of the lung are also over-cut. However, E-SRG can completely segment the lung tissue, maintain the normal position of the trachea, and there is no excessive segmentation of blood vessels and trachea. It can be seen from the experimental results that E-SRG can completely segment the object and background in the image, and can achieve good segmentation effect, which meets the realistic visual needs. Through the above comparison, it can be found that the E-SRG algorithm can automatically and objectively select the seed regions in the image, and can achieve better visual effects, which is suitable for the segmentation of medical images with high gray level. In addition, the segmentation of E-SRG does not depend on the pixel labeling and size of the image, nor does it need to train and optimize the complex network, so it can meet the processing requirements of medical images.

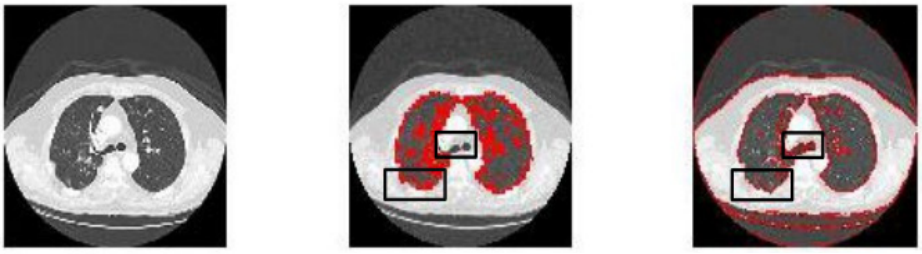

(a) Pre-processed CT image

(b) SRG segmentation diagram

(c) E-SRG segmentation diagram

Figure 5 Schematic representation of the segmentation results

4. Concluion

With the new artificial intelligence technology, traditional medicine is developing towards the direction of intelligence. In the process of smart city construction, how to combine science and technology with traditional industry organically is an urgent problem to be solved. In the field of computer vision, image processing and recognition technology is one of the key technologies. In this paper, according to the unique pathological characteristics of medical images and the requirements of medical diagnosis, the application of traditional segmentation and recognition methods in medical images is analyzed. In terms of medical image quality, this paper proposes an efficient convolution algorithm.

Reference

[1] Zhang X., Zeng Y., Lin F., Hu C., Xu C., Li T., Zhao S., Wei W. and Zhang X. (2021) Quantification of hormone levels in patients with coronavirus disease 2019 by lung CT image volumetry software. International J Respiratory, 41(17):1297-1304.

[2] Liu S., Zeng Z., Ao F., Xie X., He H. and Chen G. (2021) Application of artificial intelligence technology to analyze the characteristics of lung CT imaging in patients with newly diagnosed COVID-19. Journal of Hubei University of Medicine, 40(03): 273-276+280.

[3] Wang P., Gong Y. and Sun D. (2021) Effect of CT imaging three-dimensional reconstruction puncture combined with ablation therapy on biopsy rate and quality of life in patients with lung tumors. Chin J CT & MRI, 19(04): 60-63.

[4] Shan S., and Guo C. (2020) Value of CT imaging features of pulmonary ground glass nodules in evaluating the invasiveness of lung adenocarcinoma. Clinical Research, 28(09): 10-11.

[5] Zhang Y., Jiang H, Mao X., Pan Y. and Ma Y. (2018) Application of Myrian image post-processing system in the diagnosis of early lung cancer in elderly patients. Chin J Multiple Organ Diseases in the Elderly, 17(10): 735-739.

[5] Zhang Yinwen, Jiang Hao, Mao Xiaobo, Pan Yanan, Ma Yongfeng. The application of Myrian image post-processing system in the diagnosis of early lung cancer in the elderly [J]. Chinese Journal of Multi organ Diseases for the Elderly, 2018,17 (10): 735-739

[6] Li Jiayu, Zuo Haoxin, Zheng Yan, et al COVID-19 detection system based on deep learning and lung CT [J] Computer Programming Skills and Maintenance, 2022 (7): 106-108111

[7] Ren Hailing, Zhou Tao, Huo Bingqiang Computer aided diagnosis model of lung tumor imaging based on integrated DE-NRS [J] Computer Application and Software, 2020, 37 (5): 156-163204

[8] Wang Hailing, Fan Yingle, Chen Ke, et al Low dose lung CT image enhancement based on FHN neuron stochastic resonance [J] Aerospace Medicine and Medical Engineering, 2012,25 (2): 121-125

[9] Zheng Xiangpeng, Hua Yanqing, Lu Chen, et al Early Imaging Study of Experimental Idiopathic Pulmonary Fibrosis: Establishment of Animal Model [J] Shanghai Medical Imaging, 2001,10 (2): 137-140

[10] Wang Yang, Li Jianfeng SSD pulmonary nodule detection method combined with depth residual network [J] Journal of Jiamusi University (Natural Science Edition), 2020, 38 (6): 96-100117